

Transition of a nanomechanical Sharvin oscillator towards the chaotic regime

This content has been downloaded from IOPscience. Please scroll down to see the full text.

2017 New J. Phys. 19 033033

(<http://iopscience.iop.org/1367-2630/19/3/033033>)

View [the table of contents for this issue](#), or go to the [journal homepage](#) for more

Download details:

IP Address: 143.248.221.120

This content was downloaded on 06/04/2017 at 06:46

Please note that [terms and conditions apply](#).

You may also be interested in:

[Self-excitation in nanoelectromechanical charge shuttles below the field emission regime](#)

F Rütting, A Erbe and C Weiss

[Synchronizing a single-electron shuttle to an external drive](#)

Michael J Moeckel, Darren R Southworth, Eva M Weig et al.

[Self-sustained oscillations in nanoelectromechanical systems induced by Kondo resonance](#)

Taegeun Song, Mikhail N Kiselev, Konstantin Kikoin et al.

[Large parametric amplification in an optomechanical system](#)

F M Buters, H J Eerkens, K Heeck et al.

[Non-linear dynamics of semiconductor superlattices](#)

Luis L Bonilla and Holger T Grahn

[Topical review: spins and mechanics in diamond](#)

Donghun Lee, Kenneth W Lee, Jeffrey V Cady et al.

[Tunable coupled nanomechanical resonators for single-electron transport](#)

Dominik V Scheible, Artur Erbe and Robert H Blick

[A capacitive silicon resonator with a movable electrode structure for gap width reduction](#)

Nguyen Van Toan, Masaya Toda, Yusuke Kawai et al.



PAPER

Transition of a nanomechanical Sharvin oscillator towards the chaotic regime

OPEN ACCESS

RECEIVED

10 October 2016

REVISED

15 January 2017

ACCEPTED FOR PUBLICATION

7 March 2017

PUBLISHED

27 March 2017

Original content from this work may be used under the terms of the [Creative Commons Attribution 3.0 licence](#).

Any further distribution of this work must maintain attribution to the author(s) and the title of the work, journal citation and DOI.



Joon Hyong Cho¹, Minah Seo¹, Taikjin Lee¹, Jae Hun Kim¹, Seong Chan Jun², Young Min Jhon¹, Kang-Hun Ahn³, Robert H Blick⁴, Hee Chul Park⁵ and Chulki Kim¹

¹ Sensor System Research Center, Korea Institute of Science and Technology, Seoul 02792, Republic of Korea

² Department of Mechanical Engineering, Yonsei University, Seoul 03722, Republic of Korea

³ Department of Physics, Chungnam National University, Daejeon 34134, Republic of Korea

⁴ Center for Hybrid Nanostructures, Universität Hamburg, Falkenried 88, Hamburg D-20251, Germany

⁵ Center for Theoretical Physics of Complex Systems, Institute for Basic Science, Daejeon 34051, Republic of Korea

E-mail: hcpark@ibs.re.kr and chulki.kim@kist.re.kr

Keywords: nanoelectromechanical system, impact oscillator, chaos

Supplementary material for this article is available [online](#)

Abstract

We realize a nanomechanical *impact oscillator* driven by a radiofrequency signal. The mechanical impact of the oscillator is demonstrated by increasing the amplitude of the external radiofrequency signals. Electron transport in the system is dramatically modified when the oscillator is strongly driven to undergo forced impacts with electrodes. We exploit this nonlinear kind of electron transport to observe the current response in the chaotic regime. Our model adopting the Sharvin conductance at the moment of impact provides a description of the rectified current via the impact oscillator in the linear regime, revealing a path towards chaos.

Impact oscillators are an important class of discrete dynamical systems where an oscillator is driven under intermittent or periodic contacts with limiting constraints [1–5]. Although these oscillators show typically linear response, the boundary conditions introduce nonlinearity into the system. Studies on the nonlinear behavior of impact oscillators have proliferated on different size scales from offshore engineering, where ships collide with fenders [6], to other practical examples of oscillatory systems such as rattling gears, vibration absorbers, and impact print hammers [7–9]. Recent progress in nanotechnology provided tools to fabricate systems in which mechanical degrees of freedom play an important role in charge transfer, such as single electron shuttles, where an oscillating metallic island impacts with electrodes [10–12]. However, thorough consideration of mechanical impact on the micro- and nanoscale systems has been hindered so far by the limited control of parameters and measurement resolution.

A nanomechanical electron shuttle is an electromechanical coupler which is usually characterized by mechanically modulated currents; the shuttle transfers electrons from one electrode to the other via mechanical oscillations [10–19]. The electron shuttle consists of a nanomechanical resonator supporting a metallic island which oscillates between two electrodes. This operation principle naturally suppresses co-tunneling events in electron transport, thus enabling to control the current in the single electron limit even at room temperature [10, 17, 20]. Like for the classical pendulum the driving amplitude and frequency of the nanomechanical oscillator can be tuned by an external radiofrequency source. It was found that when it is driven by a time-dependent bias voltage the electron shuttle operates as a nanomechanical rectifier at fractional frequencies of the fundamental mode [21, 22]. This rectification is attributed to a nonlinear response of the shuttle.

The question arising now is whether an electron shuttle experiencing mechanical impacts—traced in electron transport—against the electrodes, leads to a fundamentally different nonlinear kind of electron transport. This was discussed already in [11] where single electron shuttles having contacts with source or drain are driven by ultrasonic waves. More recently, it was reported that synchronization of the electron shuttle to an external drive could be realized assuming inelastic impact events at its maximum displacements [12]. Along this line of thought, we are investigating the nonlinear current response of a nanomechanical impact

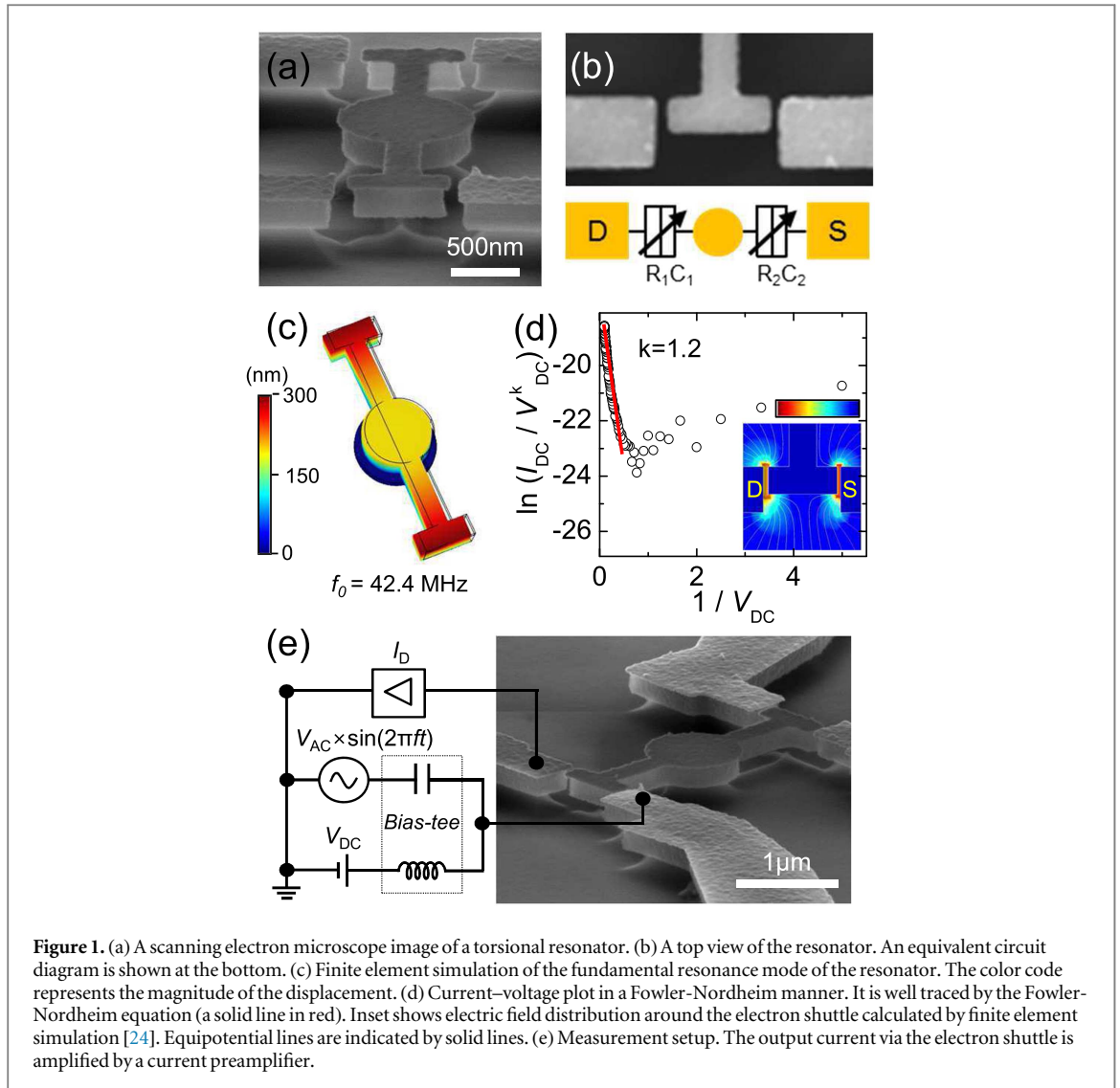
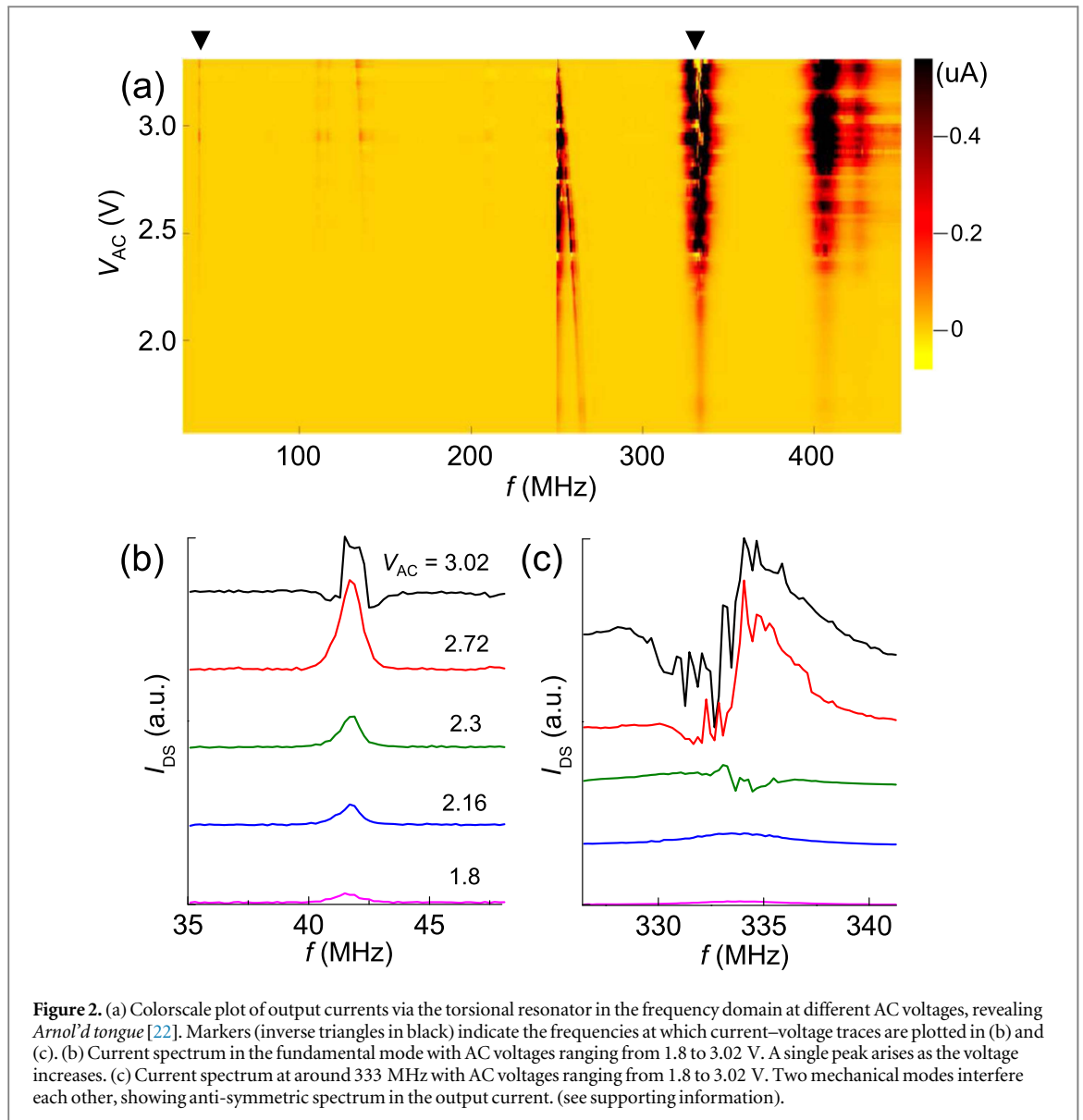


Figure 1. (a) A scanning electron microscope image of a torsional resonator. (b) A top view of the resonator. An equivalent circuit diagram is shown at the bottom. (c) Finite element simulation of the fundamental resonance mode of the resonator. The color code represents the magnitude of the displacement. (d) Current–voltage plot in a Fowler–Nordheim manner. It is well traced by the Fowler–Nordheim equation (a solid line in red). Inset shows electric field distribution around the electron shuttle calculated by finite element simulation [24]. Equipotential lines are indicated by solid lines. (e) Measurement setup. The output current via the electron shuttle is amplified by a current preamplifier.

oscillator—coined Sharvin oscillator—driven by a radiofrequency signal. Interestingly, the current via the system is dramatically modulated by the mechanical impacts of the oscillator. For this, we suggest a theoretical model which reproduces the characteristic features of the rectified currents in different regimes, revealing a path toward chaos.

An electron shuttling system is realized in the form of a torsional resonator designed in such a fashion that the center of mass of the system stays fixed to minimize the dissipation [23]. It is fabricated out of an intrinsic silicon wafer in which a 300 nm thick silicon dioxide layer is thermally formed. An amorphous silicon layer with 200 nm thickness was deposited on top of the insulating layer using plasma-enhanced chemical vapor deposition. The resonator is defined by an electron beam lithography and Ti/Au layers (10/70 nm) are thermally deposited, providing a conduction path. The patterned gold layer works as an etch mask in reactive ion etching. This leads to form a body of the resonator on the substrate by selectively etching out the amorphous silicon layer down to the silicon dioxide layer. Then the whole structure is immersed in buffered oxide etch solution to remove the sacrificial layer of the silicon dioxide underneath the arms of the resonator. For this, the etch rate for the silicon dioxide has been engineered precisely in order to make sure that the pivot in the resonator remains with 200 nm in diameter.

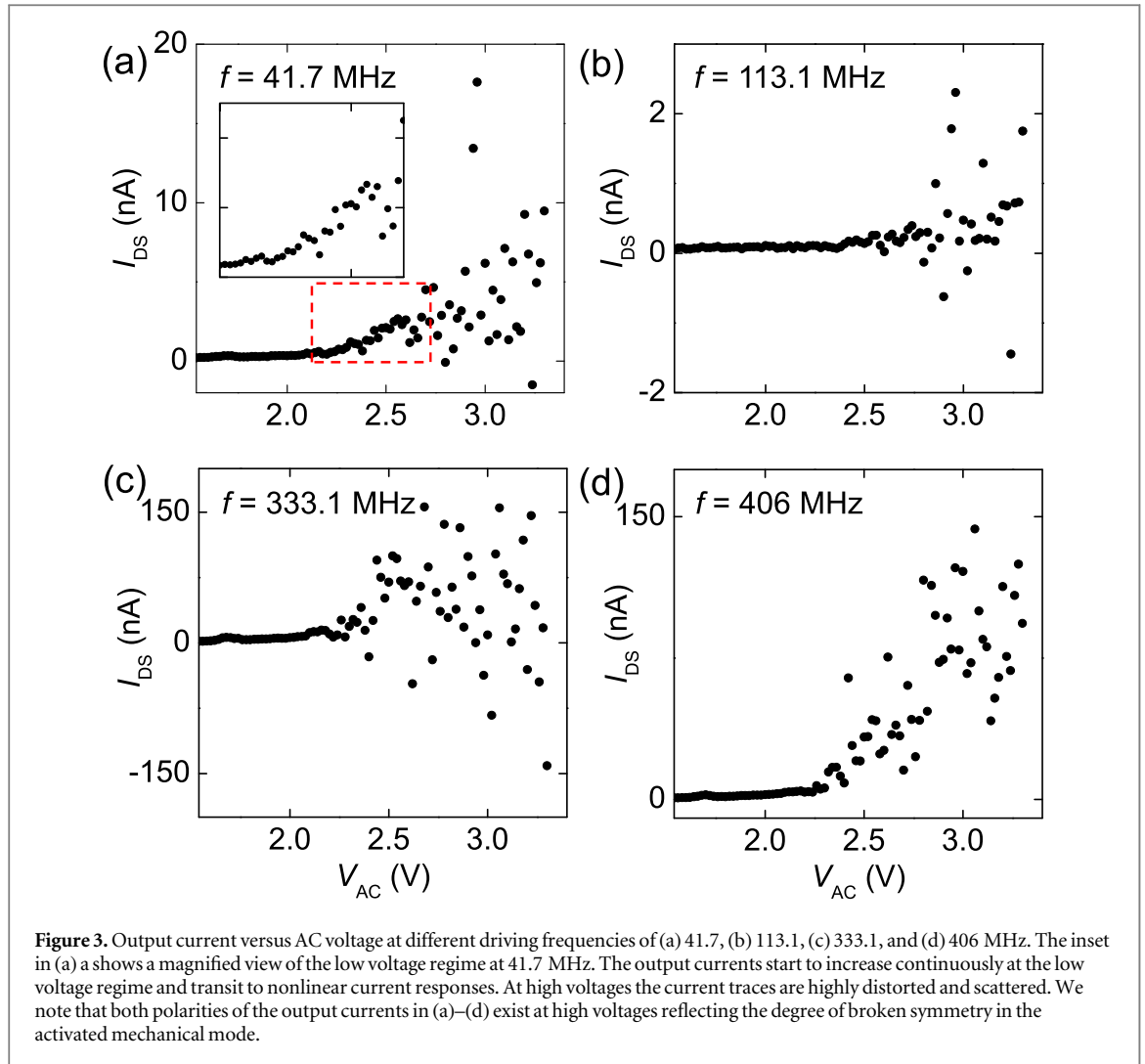
Both oscillating arms have dimensions of $1.5 \mu\text{m}$ in length and 250 nm in width. A shuttle at the tip oscillates between two electrodes (see figures 1(a) and (b)). A schematic diagram of an equivalent circuit for the electron shuttle is shown in the bottom of figure 1(b) which is comprised of tunable resistances and capacitances. The gap distances between the resonator and electrodes are in the range of 25 and 40 nm. All the following measurements were performed in a probe station equipped with RF (DC to 40 GHz) probes under vacuum ($\leq 10^{-5}$ Torr) at room temperature. The electromechanical response of the shuttling system under external bias voltages is investigated with the measurement configuration shown in figure 1(e) where external DC and AC voltage sources can be superimposed via a bias tee. The direct current via the shuttle is amplified in a current



preamplifier. The threshold voltages in both directional currents are different reflecting the asymmetric configuration of the shuttling system in terms of the gap distances towards both electrodes. The electric field distribution around the electron shuttle under the DC bias voltage of 1 V is calculated where strong field enhancement is apparent due to the proximity of the shuttle and electrodes (see the inset of figure 1(d)) [24]. Plotting the data in the Fowler-Nordheim manner manifests the nonlinear current response at different DC voltages where the linear slope at high voltages is observed using the exponent, k of 1.2 in the Fowler-Nordheim equation ($k = 2$ is the original constant) (see figure 1(d)) [25, 26].

Now we explore the mechanical response of the electron shuttle in the frequency domain. Finite element simulation allows us to estimate the fundamental mode to be at around $f = 42.4$ MHz (see figure 1(c)) [24]. The calculated displacement of the shuttle shows that it is highly possible for the shuttle to make contacts with electrodes in resonance considering the formed gap distances. As described in [21], nonzero rectified currents via the electron shuttle with asymmetric configuration under AC voltages (zero DC bias voltage) are monitored (see the measurement setup in figure 1(e)). The frequency of the time-dependent voltage is swept in the range of 31.3 to 450 MHz. The amplitude of the AC voltage varies from 1.54 to 3.30 V. The overall current spectra are summarized in figure 2(a). As we increase the amplitude of the applied AC voltage, the whole structure of *Arnol'd tongue* is revealed where color codes represent rectified current amplitudes in several mechanical modes of the oscillator [16, 22, 27].

The current responses at different AC voltages in the fundamental mode and a mode at the frequency of 333 MHz (marked by inverted triangles in figure 2(a)) are shown in figures 2(b) and (c). As the AC voltage amplitude increases, the rectified currents arise at resonances of the torsional oscillator. At low amplitudes of the applied AC voltages, the spectra reflect a linear behavior of the system. We note, however, that the system at the



frequency of 333 MHz has undershoots and zero crossings at higher voltages (see figure 2(c)). This becomes more pronounced as the AC voltage increases, starting out at the voltage of about 2.2 V. This stems from the interference between two adjacent mechanical modes since the coupling between two mechanical modes increases at high voltages (see supplementary information).

Our key result is that the obtained current spectrum is distorted and the current via the torsional resonator in the high voltages appear scattered. Current traces for various mechanical modes are presented in figures 3(a)–(d). Although the threshold voltages for the exponential increase and the following scattered currents are different depending on the chosen mechanical modes, they start to appear in the range of 2.3 to 2.7 V. The inset in figure 3(a) shows a magnified view of the transition point according to the applied AC voltage. It is apparent that increasing the AC voltage across the resonator brings the system into a nonlinear regime. We note that both polarities of the scattered output currents exist at high voltages reflecting the broken symmetry in the activated mechanical mode [16, 21, 22]. This observation, which we back up with theoretical consideration to follow, implies that the electron shuttle having intermittent or periodic impacts with electrodes experiences transitions towards a chaotic regime in the current response.

We suggest a theoretical model to obtain a better understanding of the obtained results where a nanoelectromechanical shuttle is assumed to be a damped harmonic oscillator with the fundamental mode at the frequency, f_0 . In the model we are considering a situation where the parametric resonance under time-dependent driving leads to mechanical impacts towards electrodes at high voltages. Essential for this model are the additional external driving forces, $F_e(x(t); t)$ and $F_b(x(t))$. The equation of motion between the electrodes reads

$$m\ddot{x}(t) + m\gamma\dot{x}(t) + m\omega_0^2x(t) = F_e(x(t); t) + F_b(x(t)), \quad (1)$$

where m is the effective mass of the oscillator, γ is a dynamic damping parameter, and ω_0 is the eigenfrequency of the oscillator. The system is driven by an electrostatic force, $F_e(x(t); t) = -Q(x(t); t)V(t)/L$, where $Q(x(t), t) = CV(t)\tanh(x(t)/\xi + \alpha)$, and $V(t) = V_{AC}\sin(\omega t)$ (C is the junction capacitance, L is the gap

distance between the electrodes, ξ is the characteristic tunneling length, and $\alpha = 1/2\ln(R_{r0}/R_{l0})$ represents the geometric asymmetry). Two electrodes are located at positions $x = \pm \frac{L}{2}$ and restrain its oscillation such that elastic impacts occur. The elastic bouncing force is described by $F_b(x(t)) = -\gamma_b h(x(t))^{3/2}$, with $\gamma_b = \frac{2}{3} \frac{E}{1-\sigma^2} \sqrt{\frac{R}{2}}$ (R is the radius of the shuttle, σ is the Poisson's ratio, and E is the Young's modulus.), and the deformation distance, $h(x(t)) = \bar{x}(x(t))\Theta(\bar{x}(x(t)))$ ($\bar{x}(x(t)) = |x(t)| - L/2$, and $\Theta(z)$ is the Heaviside step function.) [28].

The time-averaged rectified current is calculated as

$$I_{\text{DC}} = \int \left[\frac{V_{\text{AC}}}{2R_0} \operatorname{sech}\left(\frac{x(t)}{\xi} + \alpha\right) \sin(\omega t) + I_c(x(t); t) \right] dt, \quad (2)$$

with $R_0 = 2\pi\hbar/2e^2$ as resistance unit, and the contact current, $I_c(x; t)$. Assuming the Sharvin model for the contact conductance with the detail in supplementary materials, the contact current is described as

$$I_c(x(t); t) = \frac{V_{\text{AC}}}{2R_0} \sum_j D_j(x(t)) \sin(\omega t), \quad (3)$$

with $D_j(x(t)) = \frac{G_j(x(t))(1 - \frac{1}{2}e^{L/2\xi} \operatorname{sech}(L/2\xi - \alpha))}{2(1 + G_j(x(t))R_0 e^{\mp x(t)/\xi})}$, and the Sharvin conductance, $G_j(x(t)) = \frac{\pi^2 (R - h(x(t)) / 4) h(x(t))}{R_0 \lambda_F^2}$ (λ_F is the Fermi wave length.) [29]. When the amplitude of the oscillation is small enough, $|x|/\xi \ll 1$, equation (1) can be reduced into the damped Mathieu equation [30]. The principal instability regime is then obtained by solving the equation with two variable expansion method.

The calculated currents based on the suggested model as above are plotted in the plane of frequencies and AC voltages in figure 4(a). We find a principal instability regime, $V_- \leq V \leq V_+$, where

$$V_{\pm}(\omega) = \sqrt{\frac{2m\omega_0^2 \lambda L}{C}} \sqrt{\frac{4}{3}(\omega^2 - \omega_0^2) \pm \frac{2}{3}\sqrt{(\omega^2 - \omega_0^2)^2 - 3\gamma^2}}. \quad (4)$$

The solid line in figure 4(a) indicates the analytic results of critical voltage as a function of external frequency from equation (4). In the principal instability regime, so-called *Arnol'd tongue*, the parametric amplification causes the instability of the shuttling system and the motion is mode-locked in the dressed resonance frequency, $\Omega_0 = \sqrt{\omega_0^2 + \frac{C V_0^2}{2\lambda m L}}$. The environmental damping shifts the critical transition point of the bifurcation with modified edges in the *Arnol'd tongue*. The *Arnol'd tongue* is divided into three regions: a continuously varying current region, a scattered current region, and a region having both features (see figures 4(a) and (b)). The current trace at $\omega/\omega_0 = 1.05$ is shown in figure 4(b). Different states along the applied AC voltages are apparent in the current–voltage curve where the transition points correspond to the position of dots in figure 4(a). They are a conventional shuttling state (US1), a shuttling state with periodic impacts where the oscillator is synchronized with the driving source (US2), and a chaotic shuttling state with irregular impacts (US3). Corresponding states of the electron shuttle are schematically described in figures 4(c)–(e). The current trace begins with a monotonic increase in the low voltages mainly due to the geometric asymmetry (see a magnified view of the low voltage regime in the inset of figure 4(b)), while it is known that the electron shuttle in a symmetric probing configuration gives rise to zero DC current under external AC voltages [22]. The shuttle in this state (US1) shows a periodic oscillation without collisions with electrodes. The electrons transfer only when the shuttle is displaced sufficiently for electrons to tunnel into electrodes in proximity. In the following state (indicated as US2 in figure 4(b)) the oscillation of the shuttle is synchronized with the external AC voltage at integer-multiples of the fundamental mode frequency and has regular impacts with the electrodes. Here, the current increases exponentially unlike the conventional shuttling state. Finally, scattered currents appear at the higher voltages (indicated as US3 in figure 4(b)). We identify the theoretically encountered states of the electron shuttle by matching the calculated current with the experimental one. The critical voltage and current levels as well as the transition toward the scattered current are in agreement with the experiment despite of the difficulty in quantifying the environmental parameters of the structure at the nanoscale (i.e. parameters given in the caption of figure 4(b)). Hence, our model adopting the Sharvin conductance at the moment of impact provides a good description of the rectified current via the Sharvin oscillator.

The Lyapunov exponents are calculated along with the AC voltages as shown in figure 4(f). We note that the Lyapunov exponents become positive in the scattered current state implying that long-term prediction becomes impossible in this regime where small uncertainties are amplified fast. The calculated displacement shows highly irregular impacts with both electrodes (see figure 4(g)). More insight can be gained from a Poincaré section. The Poincaré section in this regime is partially filled reflecting the complexity of the system induced by those impact events (see figure 4(h)) [3, 4]. The successive points are found to hop chaotically over the attractor, exhibiting sensitive dependence on the initial conditions as typically expected in a chaotic state. Since the duration of the contact is sufficiently short compared to the period of the oscillation, impacts can be assumed to be momentary

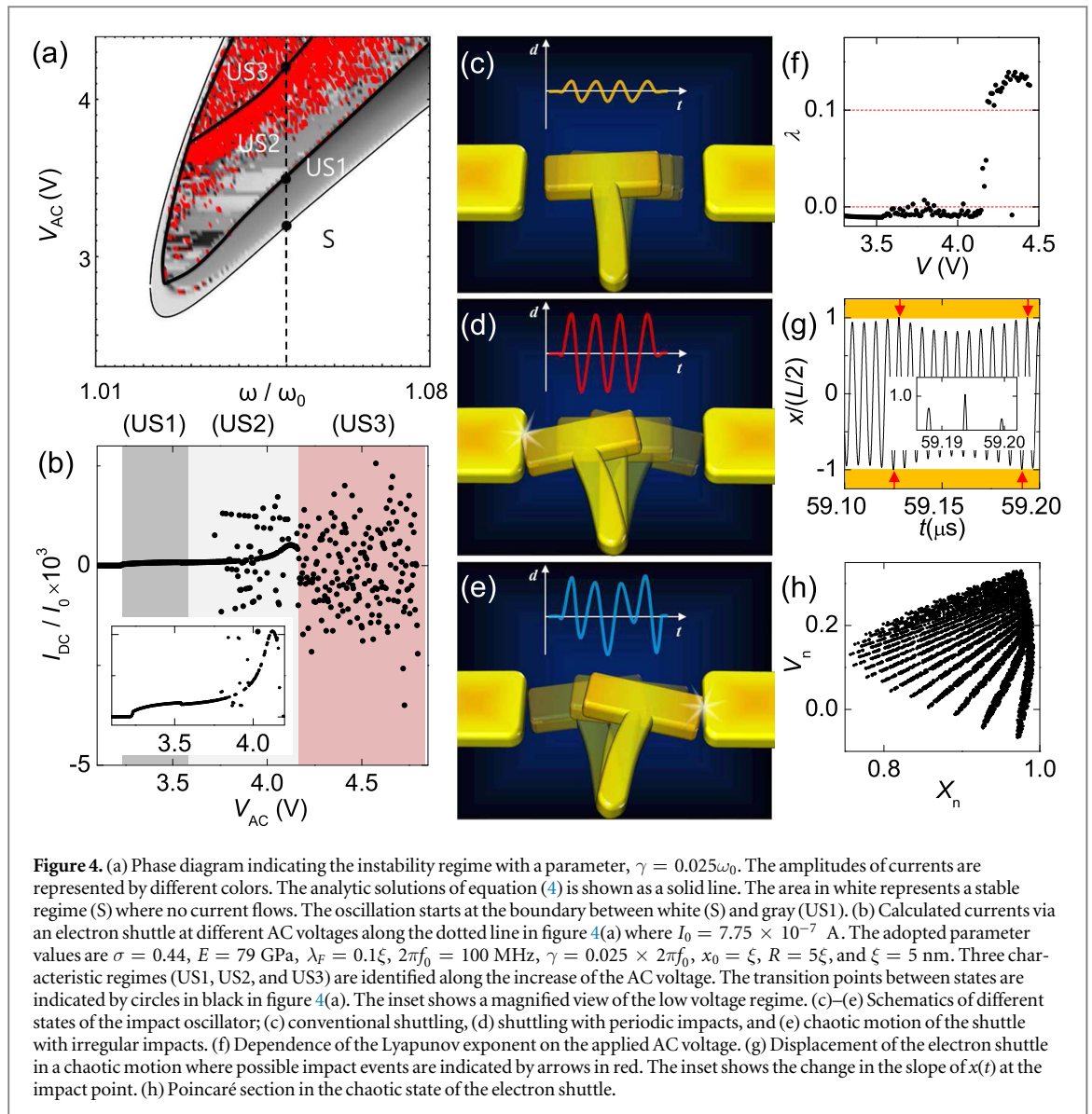


Figure 4. (a) Phase diagram indicating the instability regime with a parameter, $\gamma = 0.025\omega_0$. The amplitudes of currents are represented by different colors. The analytic solutions of equation (4) is shown as a solid line. The area in white represents a stable regime (S) where no current flows. The oscillation starts at the boundary between white (S) and gray (US1). (b) Calculated currents via an electron shuttle at different AC voltages along the dotted line in figure 4(a) where $I_0 = 7.75 \times 10^{-7}$ A. The adopted parameter values are $\sigma = 0.44$, $E = 79$ GPa, $\lambda_F = 0.1\xi$, $2\pi f_0 = 100$ MHz, $\gamma = 0.025 \times 2\pi f_0$, $x_0 = \xi$, $R = 5\xi$, and $\xi = 5$ nm. Three characteristic regimes (US1, US2, and US3) are identified along the increase of the AC voltage. The transition points between states are indicated by circles in black in figure 4(a). The inset shows a magnified view of the low voltage regime. (c)–(e) Schematics of different states of the impact oscillator; (c) conventional shuttling, (d) shuttling with periodic impacts, and (e) chaotic motion of the shuttle with irregular impacts. (f) Dependence of the Lyapunov exponent on the applied AC voltage. (g) Displacement of the electron shuttle in a chaotic motion where possible impact events are indicated by arrows in red. The inset shows the change in the slope of $x(t)$ at the impact point. (h) Poincaré section in the chaotic state of the electron shuttle.

and periodic events. With this, we find similarities between the observed transition in our system and the one in the classical kicked oscillator model [31].

In conclusion, our experiment demonstrates how impacts affect the current via a nanomechanical oscillator. We fabricated a torsional resonator which oscillates between two electrodes. Under the application of a time-dependent bias voltage a nonzero rectified current is observed at resonance frequencies. The presented system stands out by the finding that the electron shuttling under impacts provides with highly nonlinear current. A theoretical model for the system assuming mechanical impact and Sharvin conductance is suggested and it reproduces well the experimentally obtained currents via the shuttle. Furthermore, the suggested model predicts the evolution of the current via the torsional resonator, revealing the possible transition towards chaos. These findings open new perspectives to investigate unexplored regimes of nanomechanical electron transport.

Acknowledgments

This work was partially supported by the KIST institutional program (Project No. 2E27270), the IBS program (Project No. IBS-R024-D1), and Basic Science Research Program through the National Research Foundation of Korea (NRF) funded by the Ministry of Education (2013R1A1A2A10013147). RHB likes to thank the Center for Ultrafast Imaging for support. HCP thanks the KIAS Center for Advanced Computation for providing computing resources.

References

- [1] Shaw S W and Holmes P 1983 *Phys. Rev. Lett.* **51** 623–6
- [2] Moore D B and Shaw S W 1990 *Int. J. Non-Linear Mechanics* **25** 1–16
- [3] Peterka F and Vacik J 1992 *J. Sound Vib.* **154** 95–115
- [4] Budd C J and Lee A G 1996 *Proc. R. Soc. A* **452** 2719
- [5] Dyskin A V, Pasternak E and Pelinovsky E 2012 *J. Sound Vib.* **331** 2856–73
- [6] Lean G H 1971 *Trans. R. Inst. Nav. Archit.* **113** 387–99
- [7] Karagiannis K and Pfeiffer F 1991 *Nonlinear Dyn.* **2** 367–87
- [8] Sharif-Bakhtiar M and Shaw S W 1988 *J. Sound Vib.* **126** 221–35
- [9] Tung P C and Shaw S W 1988 *J. Vib. Acoust. Stress Reliab.* **110** 193–200
- [10] Gorelik L Y, Isacson A, Voinova M V, Kasemo B, Shekhter R I and Jonson M 1998 *Phys. Rev. Lett.* **80** 4526–9
- [11] Koenig D R, Weig E M and Kotthaus J P 2008 *Nat. Nanotechnol.* **3** 482–5
- [12] Moeckel M J, Southworth D R, Weig E M and Marquardt F 2014 *New J. Phys.* **16** 043009
- [13] Erbe A, Weiss C, Zwerger W and Blick R H 2001 *Phys. Rev. Lett.* **87** 096106
- [14] Scheible D V, Erbe A and Blick R H 2002 *Appl. Phys. Lett.* **81** 1884
- [15] Scheible D V and Blick R H 2004 *Appl. Phys. Lett.* **84** 4632–4
- [16] Kim C, Park J and Blick R H 2010 *Phys. Rev. Lett.* **105** 067204
- [17] Kim C, Prada M and Blick R H 2012 *ACS Nano* **6** 651–5
- [18] Kim C, Prada M, Platero G and Blick R H 2013 *Phys. Rev. Lett.* **111** 197202
- [19] Kim C, Prada M, Qin H, Kim H-S and Blick R H 2015 *Appl. Phys. Lett.* **106** 061909
- [20] Kim C, Kim H-S, Prada M and Blick R H 2014 *Nanoscale* **6** 8571–4
- [21] Pistolesi F and Fazio R 2005 *Phys. Rev. Lett.* **94** 036806
- [22] Ahn K-H, Park H C, Wiersig J and Hong J 2006 *Phys. Rev. Lett.* **97** 216804
- [23] Scheible D V, Weiss C and Blick R H 2004 *J. Appl. Phys.* **96** 1757–9
- [24] COMSOL Multiphysics, ver. 5.1, Burlington, MA, USA, 2015
- [25] Forbes R G 2008 *Appl. Phys. Lett.* **92** 193105
- [26] Kim H S, Qin H, Westphall M S, Smith L M and Blick R H 2007 *Nanotechnology* **18** 065201
- [27] Arnold V I 1983 *Russ. Math. Surv.* **38** 215–33
- [28] Landau L D and Lifshitz E M 1986 *Theory of Elasticity* vol 7 3rd edn (Oxford: Elsevier)
- [29] Sharvin Y V 1965 *J. Exp. Theor. Phys.* **48** 984–5
- [30] Butikov E I 2004 *Eur. J. Phys.* **25** 535
- [31] Tel T and Gruiz M 2006 *Chaotic Dynamics: An Introduction Based on Classical Mechanics* (New York: Cambridge University Press)